Microstructure and Mechanical Properties of Dissimilar Welds of Duplex and API Steel for Offshore Applications

T.D. Ekeh., F.T. Lawal, L.O. Osoba* and M.O.H. Amuda

Department of Metallurgical and Materials Engineering, University of Lagos, Lagos, Nigeria, 101017

* Corresponding Author: losoba@unilag.edu.ng

Abstract

Typical offshore area facilities impose stringent structural integrity and safety conditions, often necessitating dissimilar welding (DMW) for joining structural fabrication. Although various combinations of material options have been explored in service and literature, none have been able to prevent or fully justify the failure mechanism observed in the process area. In this study, DMW joints produced from duplex stainless steel (DSS) and API 5L X60 material combination using gas tungsten arc (GTA) welding process were investigated for microstructure and mechanical property evaluation using low (0.73 – 0.88kJ/mm), medium (1.3 – 1.7kJ/mm), and high (2.1 – 2.8kJ/mm) heat inputs. Microstructural characterization of the welded samples suggests the presence of a type II boundary close to and parallel to the fusion boundary close to API 5L X60 base metal. Noticeable presence of macro-segregation at the interfaces between HAZ of the base materials and the weld metal, while high heat input weldment favored the formation of delta ferrite. Morphology of the grains in the HAZ transits from coarse to equiaxed showing typical post-solidification structure with varying grain morphologies. Microhardness evaluation of the HAZ region of both DSS and X60 DMW, indicated a comparable value in all conditions with the low (262/218 HV), high (257/206 HV) and medium (235/220HV) heat inputs, respectively. In the FZ, the medium (192HV) value is intermediate between high (180HV) and low (198HV) heat inputs. The tensile and yield strength of the weldments indicated that the medium heat input has an intermediate value of 439 and 585 HV, respectively.

1. Introduction

Nigeria up until recently, is the largest oil and gas producer in Africa, with the oil and gas activities accounting for more than 98% of export earnings and about 83% of federation revenue. In addition, the oil and gas reserves concentrated in and around the Niger-Delta region generates more than 14% of the country's Gross Domestic Product (GDP) and about 65% of federal government budgetary revenues [1, 2]. As a result of marginal fields across different Oil Mining Leases (OMLs); structural platforms, rigs, networks of pipelines, piping systems, and, more recently, floating production storage and offloading (FPSO) systems are designed to transport crude and other products.

These offshore activities have led to deploying various engineering materials to produce and transport

oil and gas products successfully. These varied materials of different specifications are integrated through welding to form a whole structure.

In most oil and gas production facilities, desirable service properties that minimize occasional shutdowns and improve the integrity of structural materials are only achieved through dissimilar metal joining. The most common of such dissimilar joints are superalloy Inconel to carbon steels [3], duplex stainless steels (DSS) to carbon steels [4], and austenitic stainless steels to carbon steels [5] and many others. However, due to the high superalloy Inconel cost and its limited availability in larger diameters, carbon steels are now cladded with a layer of duplex stainless steels for crude transportation [6]. However, a major challenge in this

design is that cladding introduces specification breaks which acts as points for the initiation of failure [7]. Aside, there is a need to provide alternatives to flanges for joining dissimilar materials in offshore process areas. These twin imperatives could possibly be addressed through the innovative use of dissimilar metals weld between DSS (deployed in flow lines and gas export lines) and API 5L X60 materials, used at the cooler ends of the flow lines for economic reasons [8]. Such dissimilar metal welds are known not only to offer economic benefits but equally confer additional improved strength and better corrosion resistance [8].

Although previous studies indicate that some dissimilar welds of these materials have been implemented for various service scenarios, none of these was related to a typical offshore service area of concern in the current study [9, 10]. Laser welding has been well deployed for dissimilar metal welding, but the process is expensive and requires a higher level of technical competence to produce defect-free welds. Unlike laser welding, GTA welding process, owing to its moderate power density and economics, is an attractive process for deploying dissimilar welds. In previous studies, factors affecting microstructure-property relationship in dissimilar welds of various metallic materials have been identified but none was related to a dissimilar metal weld of DSS and API 5L X60 material, particularly for the offshore process areas; as such, there is a lack of residual information that can serve as a guide in specifying welding procedure for such specification combination [11, 12]. The problems associated with fusion welding of dissimilar joints vary and some of these challenges include residual stress problems [13] and corrosion [14 - 16] in addition to metallurgical challenges of porosity, micro-segregation, solidification cracking, non-uniform hardness distribution [17] and precipitation of secondary phases. These problems do arise due to the differences in chemical compositions, thermal properties and physical properties of the mating materials. The compositional difference in the base and filler materials is one of the prominent reasons for elemental micro-segregation and non-uniform hardness distribution in dissimilar welds, as investigated by [17 - 18]. In their studies, Manlandan et al. [19] and Ferguson et al. [20] differently established that the difficulty in producing defect-free dissimilar welds DSS and API 5L X60, irrespective of the welding technique is attributable to the noticeable differences in physical and metallurgical properties, which results in the formation of hard and brittle phases at the interface which affects the mechanical properties of such welds

[17, 21 - 22]. These phases are known as the primary reasons for failures in plants and production infrastructure [23 - 24]. The main alloying elements for DSS are chromium, nickel, molybdenum, and nitrogen [25]. It differs from conventional austenitic stainless steels in its higher chromium content (20-28%), higher molybdenum, up to 5%, lower nickel, up to 9% and 0.05-0.5% nitrogen with the potential consequential formation of secondary phases such as, sigma phase (σ), chi phase (X), laves or R-phase, Cr_2N and CrN nitrides precipitate and or Secondary austenite (γ_2) during the non-equilibrium welding process [25]. Invariably, there are still wide gaps in understanding the mechanisms driving the microstructural compositions and phase balance in dissimilar welds, which influences the structural stability of such welds.

A summarised review of a few kinds of literature on some of the associated problems common to similar and dissimilar metal weldment is presented in Table 1. Therefore, the present study attempted to contribute to unraveling better understanding via a carefully undertaken investigation of the microstructural evolution and mechanical properties in UNS32205 DSS and API 5L X60 dissimilar metal welds designed for deployment in the offshore Niger Delta process area. The scope of study entails material preparation, welding of test coupons, welding procedure qualification documentation and mechanical testing of weldments including microstructural analysis of both as received base materials and the weldments.

2. Materials and Method

### 2.1 Materials Specification and Preparation

Alloy UNS32205 (DSS) and API X60 pipes of diameter 152.4 mm and 5.5 mm thickness were the chosen base materials. Filler metal ERNiCrMo-3 is deployed for the welding of the coupons using GTA welding process. The base materials and consumables were locally sourced from some Oil and Gas companies in Nigeria with standard compositional analyses performed on the sample using Spectromaxx LMF06 with spark analyzer Pro MaXx version 1.02.001 software (Ametek, Germany) and the result of chemical composition is presented in Table 2.

Table 1 Common Problems Associated with Fusion Welding of Dissimilar joints.

No.	Authors	Inferences	Problems Identified
1	Mukherjee et al., 2018 Residual stresses and distortion in additively manufactured compositionally graded and dissimilar joints.	Graded dissimilar joints of 2.25Cr-1Mo steel alloy 800H and Ti-6Al-4V 800H were fabricated using laser-assisted powder based direct energy deposition process were examined.	Residual stress problems
2	Orhorhoro et al., 2018 Evaluation of the effect of tempering on the corrosion susceptibility of low carbon steel in sea water.	Effect of tempering on the corrosion susceptibility of machined low carbon steel in seawater was evaluated in the as received, water-tempered, oil-tempered and brine-tempered conditions at tempering temperature of 700ºC and exposure to 1000 ml of seawater collected from Niger Delta Area of Nigeria for a period of 100 days.	Corrosion problems
3	Vashishtha et al., 2017 Effect of welding processes on microstructural and mechanical properties of dissimilar weldments between conventional austenitic and high nitrogen austenitic stainless steels.	Dissimilar weldments between conventional and high nitrogen stainless steel was prepared using gas tungsten arc welding and shielded metal arc welding processes. The weld defects and their integrity were investigated by radiographic analysis. The effect of welding speeds on microstructural characteristics and grain boundary precipitation was analyzed and the consequent effect on mechanical properties was studied using tensile test and microhardness evaluation.	Elemental Micro Segregation affect mechanical properties
4	Manladan et al. (2017) A review on resistance spot welding of aluminium alloys	Resistance spot welding (RSW) of of similar and dissimilar Al/Al alloys, Al alloys/steel, Al/Mg alloys, and Al/Ti alloys, with focus on structure, properties, and performance relationships including weld bonding, effect of welding parameters on joint quality and metallurgical defects were investigated	Elemental Micro segregation affect mechanical properties
5	Wang et al., 2015; Effect of welding process on the microstructure and properties of dissimilar weld joints between low alloy steel and duplex stainless steel	High-quality dissimilar weld joints using metal inert gas (MIG) welding and tungsten inert gas (TIG) welding for duplex stainless steel (DSS) and low alloy steel were compared. The mechanical, microstructure and corrosion morphology of the dissimilar weld joints were examined using SEM, EDS, micro-hardness test, tensile test, impact test , and polarization curves. Obvious concentration gradients of Ni and Cr that exit between the fusion boundary and the type II boundary contributed to much higher hardness of the weldment	Elemental Micro segregation affects mechanical properties
6	Li et al., 2014; An investigation on microstructure and properties of dissimilar welded Inconel 625 and SUS 304 using high-power CO_2 laser.	Microstructure and properties of laser deep penetration dissimilar welded Inconel 625 nickel-based alloys and SUS304 stainless steel were investigated. Weld microstructures, room temperature tensile properties and stress rupture properties, impact toughness, and hardness of dissimilar welded joints were evaluated. The experimental results showed that the microstructure of fusion zone near the fusion line in the SUS304 side was mainly cellular, whereas that near the fusion line in the Inconel 625 was predominantly columnar dendrites. Laves phases were precipitated at the grain boundary of cellular and in the interdendritic regions of fusion zone in the different form.	Elemental Micro segregation affect mechanical properties
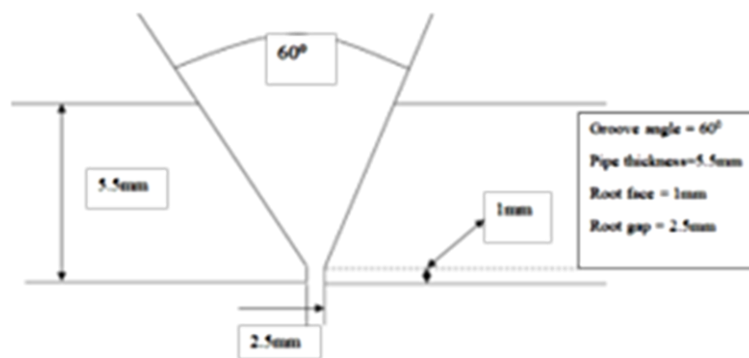
Fig. 1 Schematic illustration of the samples V- groove butt weld configurations
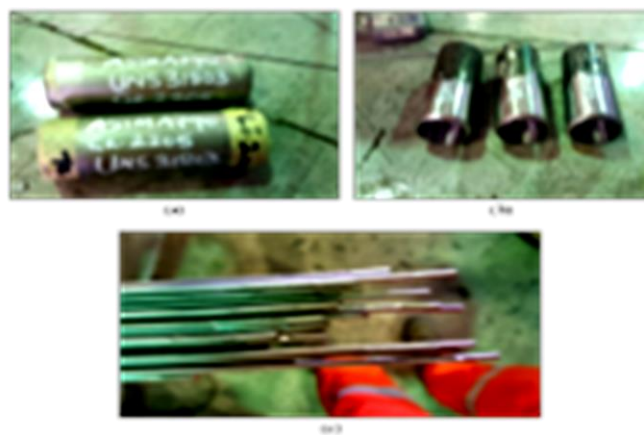
Fig. 2 Materials for the research: **(a)** DSS base material, **(b)** API 5L X60 base material and **(c)** ERNiCrMo-3 Welding consumable (Bare Rods).

Fig. 3 Experimental equipment, production process and resources used for the research: (a) Welding machine with shielding and backing gas, (b) Fit-up process and (c) Completed dissimilar welds of base metals.

2.2 Production of Dissimilar Weld Coupons

The base material samples were cut and fitted using the standard V- groove butt weld configurations as illustrated in Fig. 1. Three samples each were selected from DSS and API 5L X60 base materials (BM), with one sample from both BM welded as coupons marked W101, W102, and W103 after being visually inspected and certified free from moisture, grease, paints and other deleterious materials that could compromise the weld quality (Fig. 2). The final weld-coupons were grouped into low (0.73 - 0.88 kJ/mm), medium (1.3 - 1.7 kJ/mm) and high (2.1 - 2.8 kJ/mm) heat inputs welds as presented in Table 3. GTA Maxstar 350 welding machine, with argon as shielding gas and backing gas at 99.98 % purity and oxygen purge analyzer, was deployed in welding the pipes, which had

been previously tacking welded and held together by fit-up (Fig. 3).

Table 2: Chemical composition of base materials and filler metal

Materials						*Elemental Composition (wt. %)*						
	C	Cr	Ni	Mo	Mn	Si	Ti	Co	V	Nb	Cu	Fe
API 5L X60	0.096	0.0024	0.084	0.041	1.16	0.192	0.020	0.006	0.032	0.038	0.287	97.9
DSS 32205	0.008	22.63	5.36	3.11	1.060	0.271	0.002	0.050	0.048	0.006	0.294	66.90
ERNiCrMo-3	0.01	22.5	65.0	8.40	0.01	0.08	0.16	_	_	3.50	0.04	0.1

Table 3: Weld coupon classification

| Coupon	Number of Coupons	Heat Input Range (kJ/mm)	Heat Input Class
W101	1	0.73 - 0.88	Low Heat Input
W102	1	1.3 - 1.7	Medium Heat Input
W103	1	2.1 - 2.8	High Heat Input

After welding, the joint surfaces were made smooth and uniform and subjected to non-destructive testing involving visual inspection, radiographic testing for cracks, and checks for incomplete penetration, all by certified personnel in accordance with the requirements of the American Welding Society Certified Welding Inspectors (for visual inspection) and ASNT Level 2, CSWIP.

2.3 Microstructural and Mechanical Property Characterization

All the welds were certified free from all forms of welding defects. After that, specimens were carefully extracted from the welded pipes in the area of interest to avoid altering or destroying the structure of interest for various metallurgical and mechanical investigations, including macrostructural and microstructural analysis. Using standard metallurgical procedures, the prepared surfaces were electrolytically etched using Aqua Regia. Stereo microscope MZM + iDS Camera (Macroscope) - CK01598 and AE2000MET Microscope (Biovis Material Plus V A4.59 and Motic 2.0 software) - AE2000MET were used for the macro and microstructural evaluations. Mechanical characterizations were conducted using tensile testing in accordance with ASTM E8 standard on an INSTRON 600KN as shown in Fig. 4. The type of test, number of tests and the actual number of dissimilar welds coupons needed for the desired tests is presented in Table 4.

Fig. 4 Tensile testing of the coupons**:** (a) Pulling of the tensile specimens and (b) Ruptured tensile specimen

(a)   (b)
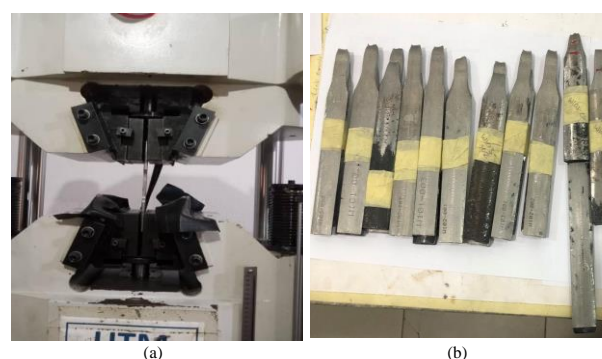
Table 4: Matrix of number of tests per weld coupons

Weld Number	Types of Mechanical Test						
	Tensile	Macro	Hardness	Micro Analysis			
Base Materials	3 Reduced section tensile	1 section	1 section				
W101	3 Reduced section tensile	1 section	1 section	Base Materials	Weld Metal	Fusion Line	HAZ
W102	3 Reduced section tensile	1 section	1 section	Ref W101	Weld Metal	Fusion Line	HAZ
W103	3 Reduced section tensile	1 section	1 section	Ref W101	Weld Metal	Fusion Line	HAZ
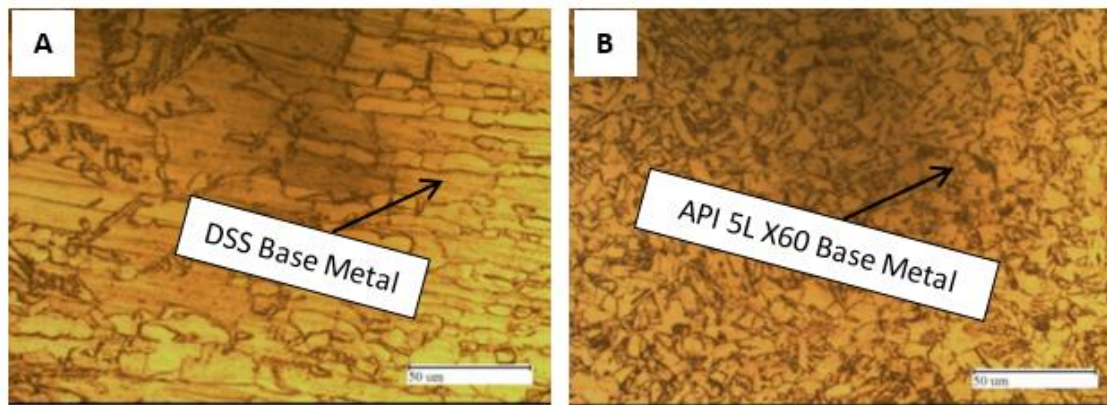
Fig. 5 (a) Microstructure of as-received DSS base metal and (b) Microstructure of as-received API 5L X60 base metal

3. Results and discussions

3.1 Microstructure of Base Materials

The microstructures of the as-received DSS and API 5L X60 base materials before GTA welding to produce dissimilar metal joints are presented in Figs. 5a and 4b, respectively. The microstructure of the DSS base material consists of austenite (light region) and ferrite (dark region) phases and an elongated grain structure arising from the effect of finishing cold manufacturing work. Similarly, the microstructure of the API 5L X60 base material shows a ferritic matrix with significant pearlite, mostly at grain boundaries. Unlike the grains' texture in the DSS, the texture in the API 5L X60 base material lacks any directional elongation, suggesting that the material was supplied in the stress-relief annealed condition.

3.2 Analysis of Weld Quality, Macrograph and Topography

Radiographic analysis of the samples shown in Fig. 6 revealed sound defect-free welds with no cracks, micro-porosity or visual weld coloration. The absence of discontinuities in the dissimilar weld coupons obtained via the radiographic examination indicates the implementation of appropriate welding procedure protocols. In essence, the combinations of process parameters considered for the production of the dissimilar welds were appropriate and adequate for forming a good quality joint which consequently may not negatively impact the mechanical properties of the joints. The weld deposit quality obtained in the present work is similar to those obtained by [26] in producing dissimilar weld joints between copper and 316L

stainless steel using the laser beam welding (LBW) process. In their work, Xin et al. [26] strengthened the joints with nickel interlayers to produce a sound weld with no welding defects or spherical particles. In another work, Mvola et al. [27] and Benyounis et al. 28] stated that welding input parameters play a very significant role in determining the quality of a weld joint, and as such, the selection of appropriate welding procedure specification is an important factor in dissimilar metal welding. The completed dissimilar weld profiles presented in Fig. 6 show a good weld profile with no visible form of distortion, indicating that the re-solidification strain in the weld arising from the thermal gradient was within the threshold for such dissimilar welds. Welds W102 and W103 had a single run capping pass, while W101 had two capping runs. As observed, There is no weld crater, undercut, lack of sidewall fusion, and burn-through on the completed coupons.

Closely related to the radiographic analysis is the macro profile of the various welds shown in Fig.7, indicating the complete penetration in the weld. The figure further validated the radiographic image of Fig. 6, showing the excellent weld fusion in the various coupons with no visible discontinuities in the dissimilar DSS and API 5L X60 welds made by GTA welding process under different heat inputs.

3.3 Microstructure of Dissimilar Welds of DSS and API 5L X60 at Different Heat Inputs

Figs. 8 - 10 show the Fusion Zone (FZ) microstructure and the HAZ boundary on both sides of the dissimilar metals at low, medium, and high heat inputs welds, respectively. Aside from the complete melting and solidification in the FZ region, there are no observable macro/microscopic re-solidification

products resulting from the peak temperature in this region. However, at the boundary region, Type II boundaries were noticeable. These are known characteristics of dissimilar joints close to and parallel to the FZ at the side of API 5L X60 base metal. Saedi et al. [29] observed a similar boundary type in the dissimilar joint of API 5l X60 and Grade 301S austenitic stainless steel produced using GTA technique. Such boundaries are known to occur due to allotropic transformations in the base material during solidification, which changes the nature of the fusion boundary. According to Nelson et al. [30] the key element in forming the Type II boundary is the ability of the gamma phase at the fusion boundary to migrate. This can occur, even during the relatively rapid cooling associated with non-equilibrium welding processes experienced in most fusion welds, because only short-range diffusion is required for the boundary to migrate.

Conversely, the optical micrographs indicate the presence of macro-segregation at the interfaces between HAZ of the base materials and the weld metal interface under different heat input conditions. The increasing formation of island-like areas is an example of macro-segregation that occurs due to the difference in liquidus temperature of the base materials and weld metal [9, 30]. It is further observed that increased heat input favoured the formation of delta ferrite in the matrix due to prolonged associated solidification time. The HAZ is the region where all phase transformations occur in the solid state. It is key for investigating the microstructure of the weldments under different welding heat inputs. The HAZ of the API 5L X60 base material, under low heat input conditions (Fig. 9), presupposes the presence of bainite and ferrite phases which are known to exacerbate brittle fracture [29 - 31].

Similarly, the high heat input weldment (Fig. 10) indicates the presence of pearlite and ferrite phases close to the HAZ of the API 5L X60 material, which could be attributable to the slower cooling rate the weldment experienced. It is further observed that grain
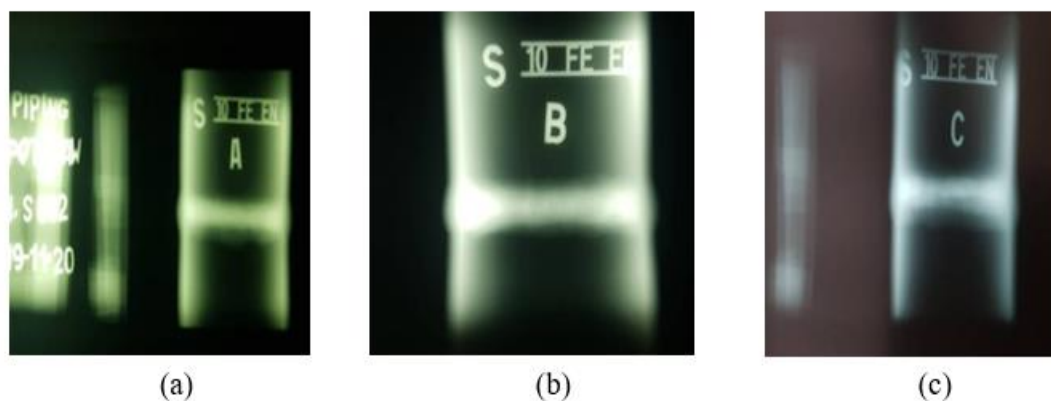
Fig. 6 Radiographs of the welded samples : (a) Weld 101 (b) Weld 102 and (c) Weld 103
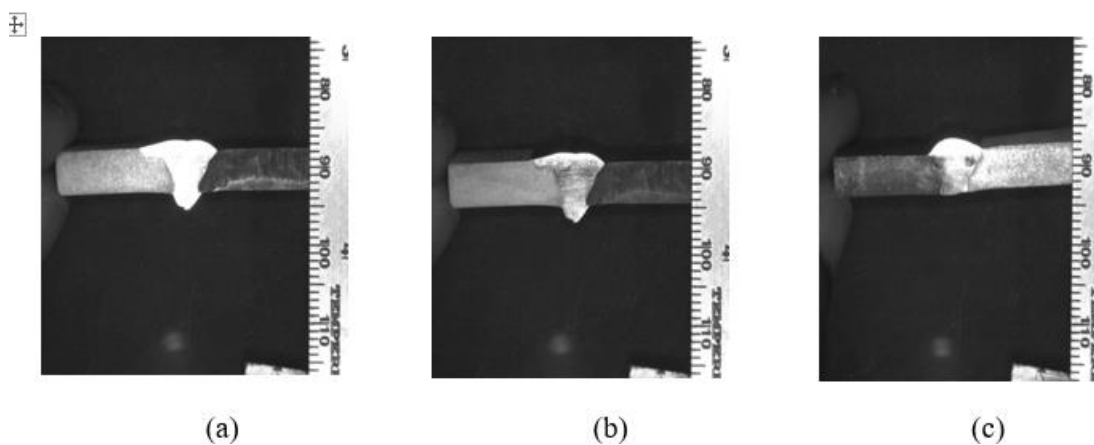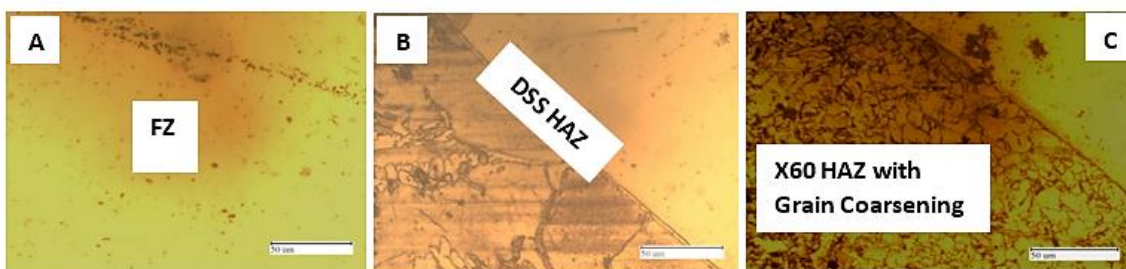

Fig. 7 Macrographs of the welded samples : (a) W101 (b) W102 and (c) W103
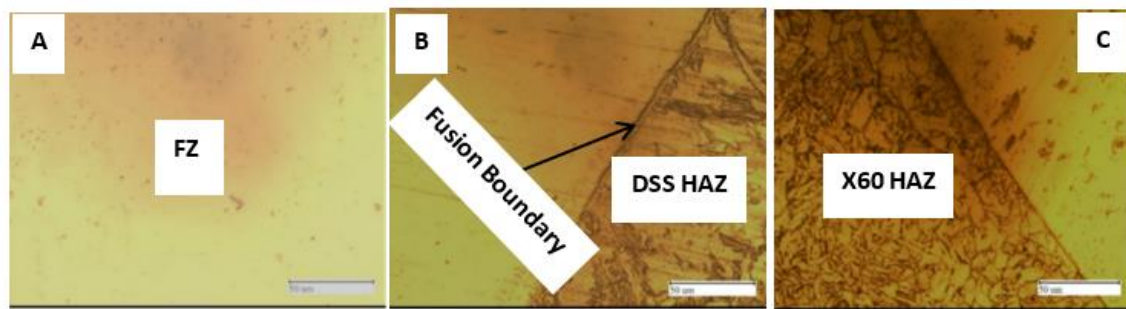
Fig. 8 Microstructures of FZ and HAZ boundary at Low Heat Input welding condition: (a) FZ, (b) DSS HAZ and (c) X60 HAZ.

Fig. 9 Microstructures of FZ and HAZ at medium heat input welding condition: (a) FZ, (b) DSS HAZ with δ ferrite island rich region and (c) X60 HAZ

Fig. 10 Microstructures of FZ and HAZ at high heat input welding condition: (a) FZ, (b) DSS HAZ with enhance grain coarsening and (c) X60 HAZ with enhance grain coarsening

coarsening close to the FZ is enhanced as the heat input is increased from low, medium, to high heat input. The HAZ microstructures depend largely on the thermal cycles and as the heat input is increased, the HAZ experiences a higher thermal impact than low heat input samples, hence the thermal cooling gradient in the higher heat input welds is reduced which inadvertently influenced the microstructures of the HAZ of both materials, leading to the formation of coarser microstructures.

3.4 Analysis of Mechanical Properties

3.4.1 Microhardness Profiles Across the Zones of the Dissimilar Coupons

The effect of heat input on the microhardness of the welded samples under low, medium, and high heat input welding in the form of hardness profile of the

different zones at different welding heat inputs is presented in Fig. 11 where evidently the high heat input welds produced the highest hardness values within the DSS and X60 HAZ, while the lowest values are obtained within the FZ, the results of which is consistent with previous investigations [16]. The heat inputs effect is more pronounced within the FZ which may have resulted in the precipitation of non-equilibrium phases arising from the differential chemistry of the two base metals in dilution with the filler metal. The FZ microstructure is severely affected by peak melting temperature and recorded the lowest hardness values compared to the HAZ of the base materials which was less affected by the peak temperature. This agrees with the findings of Kou et al. [32] who investigated the effect of heat input on the microstructure and mechanical properties of GTA

welded AISI 304 stainless steel joints. Three heat input combinations designated as low (2.563 kJ/mm), medium (2.784kJ/mm) and high heat input (3.017kJ/mm) welds were selected from the operating window of GTA welding process. Their result showed that the joints made using low heat input exhibited higher ultimate tensile strength than those welded with medium and high heat input. Significant grain coarsening due to increased heat inputs, high inter-pass temperatures, and steep cooling profiles were observed in the HAZs of all the joints. Consequently, grain coarsening in the HAZ increased with an increase in the heat input. Conversely, in the current study, the low heat input welds resulted in the lowest values of hardness observed within the base materials, however, it yielded the highest values within the FZ because of the limited time for dilution and diffusion.
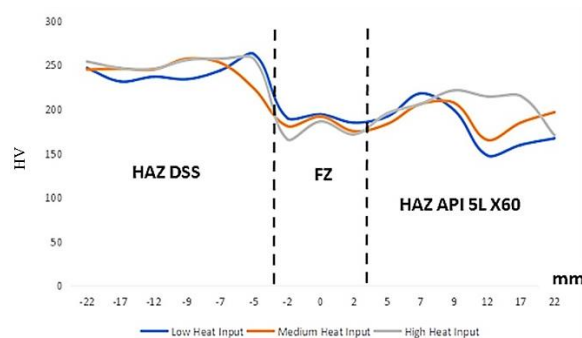
Fig. 11 Hardness profile of different zones of the weldment at different heat inputs.

It is further observed that high heat input weld produced the highest hardness values across the HAZ of both base materials due to reduced welding speed that engendered enhanced diffusion and induced re-precipitation in the partially melted region of the HAZs. Likewise, the high heat input weld had the lowest hardness values across the FZ, where complete melting and re-solidification occurred with significant dilution from the filler metal. Again, the hardness values recorded under medium heat input (intermediate between high heat input and low heat input) welds were also generally of intermediate degree in all zones of the weldment. Within the FZ, the average hardness observed falls between the high values reported for low heat input and the low values reported for high heat input.

3.4.2 Tensile and Yield Strength of Dissimilar Welded Coupons

The tensile properties of the dissimilar DSS and API 5L X60 base materials, welded under low,

medium, and high heat input welding conditions, are summarized in Table 5. Results obtained from the tensile tests conducted on the base materials expectedly indicate that the DSS base material reported a higher tensile strength of 791 MPa and a yield strength of 538 MPa, compared to the API 5L X60 base material with a tensile strength of 563 MPa and a yield strength of 445 MPa. The austenitic and ferritic dual phase of DSS and the percentage of chromium (22% and above), ensures a higher yield and tensile strength when compared to those of API 5L X60 base material. Further investigations on the tensile properties of the weldments, with specimens taken from the longitudinal section of the weldment between DSS and API 5L X60 show that the joints made under low heat input welding conditions presented a maximum tensile strength of 594 MPa and a maximum yield strength of 490 MPa.
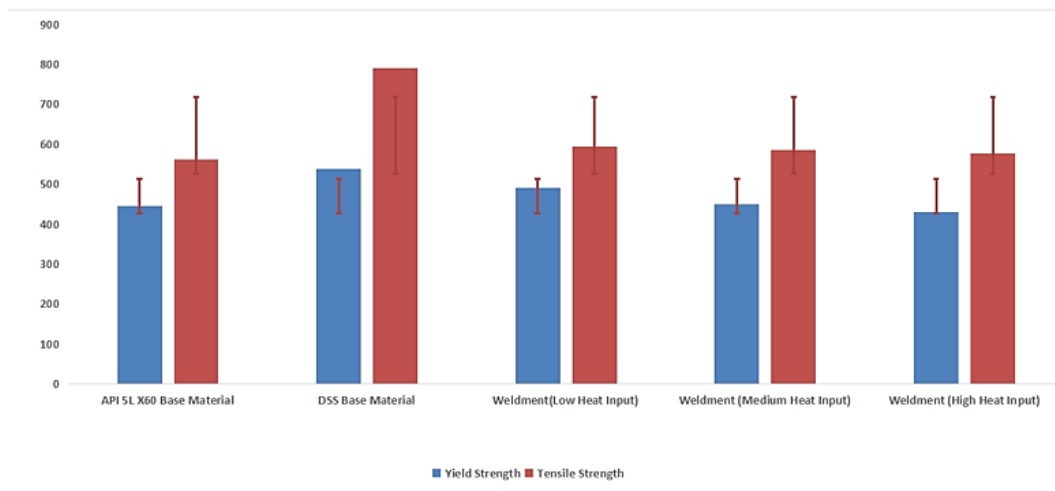
Table 5: Yield and tensile strengths of base materials and dissimilar WM at different Heat Inputs.

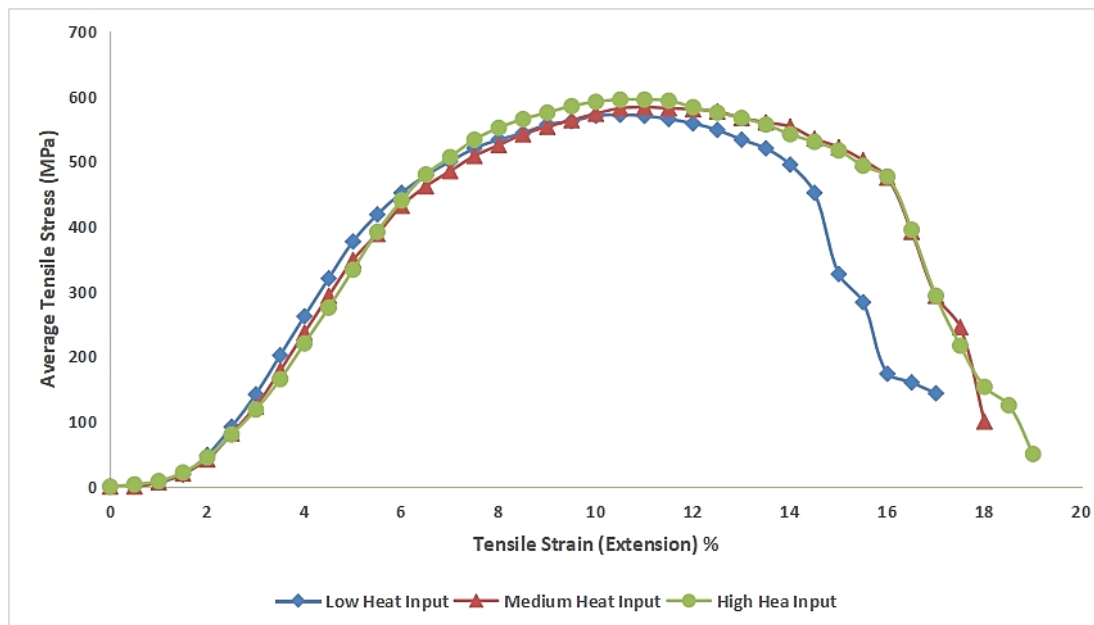| Base Material/Heat input condition	Yield Strength (MPa)	Tensile Strength (MPa)
API 5L X60 base material	445.08	562.67
DSS base material	537.96	791.30
Weldment (Low heat input)	490.58	594.35
Weldment (Medium heat input)	449.31	584.94
Weldment (High heat input)	429.80	576.73

Also, sectioned weldment from high heat input conditions, recorded the lowest tensile and yield strength of 577 MPa and 530 MPa, respectively. In comparison, the sample welded under medium heat input conditions reported a tensile and yield strength of 585 MPa and 449 MPa. Weldments under low heat input produced higher tensile and yield strength values than medium heat input, which in turn yielded higher tensile and yield strength values than high heat input weldment; thus, tensile and yield strength increased with decreasing welding heat input. This is corroborated by Subodh et al. [32]; in essence, medium heat input produced intermediate values for strength similar to the hardness profile behavior. Thus, the intermediate degree of heating, cooling, and solidification in the case of medium heat input produced structures whose tensile and yield strengths are lower than those of low heat input but higher than those of high heat input [32]. In all cases, the average yield strengths of the weldments under low, medium, and high heat input conditions are higher than those of

Table 6: Summarised Materials Data Information on DSS S32205 and API 5L X60 [33 -34].

Standard	Class	Grade		Yield Strength (MPa)	Tensile Strength (MPa)	Elongation (%)	Y.S/T.S
API SPEC 5L /ISO 3183	PSL2	L415N/X60N L415M/X60M	Min Max	415 565	520 720	≥ 25 ≥ 25	- 0.93
DSS Heat Treat - Treated	ASTM A789	Grade S32205		450	655	25	0.69

Fig. 12 Graphical representation of the Yield and Tensile strengths of Base Materials and Dissimilar Weld Metal at different Heat inputs.

Fig. 13 Graphical representation of the average stress - strain tensile properties of the Dissimilar Weld Metal at different Heat inputs.

the required minimum yield strength for API 5L X60 base material as stipulated by the API (450 MPa is the minimum required yield strength of API 5L X60 base material) Summarised materials data sheet for API 5L X60 and DSS 32205 is presented in Table 6.

This implies that the yield strength of all the welded samples can satisfy the minimum engineering application requirements for DSS and API 5L X60 dissimilar joints. For clarity and comprehension, Figures 12 and 13 summarise the graphical representation of Table 5 and the Average Stress-Strain Tensile properties of the dissimilar metal weldment, respectively.

4. Conclusions

GTA welding of UNS32205 DSS and API 5L X60 dissimilar welds for Nigeria offshore process area under different heat input conditions, using ERNiCrMo-3 filler metal, has been successfully conducted and evaluated for microstructural and mechanical behavior in environments approximating the offshore process environment with the following conclusion.

1. There are possibilities of a successful production of defect-free we ld-coupons in dissimilar materials of DSS and API 5L X60 materials using ERNiCrMo-3 filler with no form of weld coloration, distortion and a good weld profile.

2. The microhardness values obtained in the HAZ of both DSS and API 5L X60 dissimilar metal in the medium (235/220HV), Low (262/218 HV) and High heat Input welds (257/206 HV) in the current study are all comparable. Similarly in the the FZ, with the medium heat input (175HV) value intermediate between high heat input (190HV) and low heat input (170HV) .

3. The tensile and yield strength of the dissimilar weldments decreased as the welding heat input increased such that the medium heat input have an intermediate value 439 and 585 HV respectively, compare to the low heat input value of 491/594 HV and high heat input value of 430/537HV.

4. The intermediate tensile data value obtained from the medium heat inputs weldment is well above the minimum standard requirement of 415 and 520 HV for the API 5L X60 and is the recommended best condition from the current study.

5.

References

[1] I. Nwachukwu, I. C. Mbachu, The socio-cultural implications of crude oil exploration in Nigeria. *In the Political Ecology of Oil and Gas Activities in the Nigerian Aquatic Ecosystem,* Academic Press (2018) 177 – 190

[2] E.I. Seiyaboh, S,C. Izah, A review of impacts of gas flaring on vegetation and water resources in the Niger Delta region of Nigeria. *International Journal of Economy, Energy and Environment*, 2(4) (2017)**,** 48-55.

[3] C. Zhou, Q. Huang, Q. Guo, J. Zheng, X. Chen, J. Zhu,and L. Zhang, Sulphide stress cracking behaviour of the dissimilar metal welded joint of X60 pipeline steel and Inconel 625 alloy. *Corrosion Science,* 110 (2016) 242-252.

[4] Moon, B.S. Jang, S.C. Kim, and J.H. Koh, A study on characteristics of dissimilar welds between super duplex stainless steel UNS S32750 and carbon steel A516-70 with FCAW and Joining. *Journal of Welding,* 32(4)(2014) 26-33.

[5] H. Ma, G. Qin, P. Geng, F. Li, B. Fu, and X. Meng, Microstructure characterization and properties of carbon steel to stainless steel dissimilar metal joint made by friction welding. *Materials and Design*, 86 **(**2015) 587-597.

[6] X. Di, Z. Zhong, C. Deng, D. Wang and X. Guo, Microstructural evolution of transition zone of clad X70 with duplex stainless steel. *Materials and Design*, 95 (2016)**,** 231-236.

[7] C.R. Gagg, P.R. Lewis, In-service fatigue failure of engineered products and structures-Case study review. *Engineering Failure Analysis,* 16(6) (2009) 1775-1793

[8] J. Wang, M. Lu, L. Zhang, W. Chang, L. Xu, and L. Hu, Effect of welding process on the microstructure and properties of dissimilar weld joints between low alloy steel and duplex stainless steel, *International Journal of Minerals, Metallurgy, and Materials,* 19(6)(2012)**,** 518–524.

[9] H. Tasalloti, P. Kah, and J. Martikainen, Effect of heat input on dissimilar welds of ultra-high strength steel and duplex stainless steel. Microstructural and compositional analysis, *Materials Characterization,* 123 (2017) 29–41.

[10] S. Rahimi, T.N. Konkova, I. Violatos, and T.N. Baker, Evolution of microstructure and crystallographic texture during dissimilar friction stir welding of duplex stainless steel to low carbon-manganese structural steel. *Metallurgical and Materials Transactions A*, 50(2)(2019) 664-687.

[11] J. Verma, R.V. Taiwade, Effect of welding processes and conditions on the microstructure, mechanical properties, and corrosion resistance of duplex stainless-steel weldments – A review. *Journal of Manufacturing Processes,* 25(2017)134-152

[12] M.S. Khorrami, M.A. Mostafaei, H. Pouraliakbar, and A.H. Kokabi, Study on microstructure and mechanical characteristics of low-carbon steel and ferritic stainless-steel joints. *Materials Science and Engineering*: A, 608(2014) 35-45.

[13] T. Mukherjee, J.S. Zuback, W. Zhang and T. DebRoy, Residual stresses and distortion in additively manufactured compositionally graded and dissimilar joints. *Computational Materials Science,* 143(2018) 325-337.

[14] M. Vasumathi, V. Murali, S.R. Begum, and N. Rajendran, Improved corrosion resistance of carbon reinforced aluminium laminates in atmospheric environment: Roles of environment friendly jute fibre/alumina nano coating. *Journal of Polymer Materials,* 36(1)(2019)**,** 1-11.

[15] S. Won, B. Seo, J.M. Park, H.K. Kim, K.H. Song, S.H. Min, T.K. Ha, and K. Park, Corrosion behaviors of friction welded dissimilar aluminium alloys. *Materials Characterization,* 144(2018) 651-660.

[16] E. K. Orhorhoro, A. A. Erameh, and A. C. Adingwupu, Evaluation of the effect of tempering on the corrosion susceptibility of low carbon steel in sea water. Nigerian *Research Journal of Engineering and Environmental Sciences*, **3(1),** (2018) 409-415.

[17] L.O. Osoba, I.C. Ekpe, and R.A. Elemuren, Analysis of Dissimilar Welding of Austenitic Stainless Steel to Carbon Steel by TIG process, Int. Journal of Metallurgical & Materials Science and Engineering (IJMMSE) ISSN(P): 2278-2516; ISSN(E)5(5)(2015) 2278-2524. 1 -12 @IJPRC Pvt.Ltd.

[18] H. Vashishtha, R.V. Taiwade, S. Sharma, and A.P. Patil, Effect of welding processes on microstructural and mechanical properties of dissimilar weldments between conventional austenitic and high nitrogen austenitic stainless steels. Journal of Manufacturing Processes, 25(2017) 49-59.

[19] S.M. Manladan, F. Yusof, S. Ramesh, M. Fadzil, Z. Luo and S. Ao, A review on resistance spot welding of aluminium alloys. *The International Journal of Advanced Manufacturing Technology,* 90(1-4)(2017)**,** 605-634.

[20] D. Ferguson, W. Chen, T. Bonesteel and J. Vosburgh, A look at physical simulation of metallurgical processes, past, present, and future. Materials Science and Engineering, 499(1-2)(2017) 329-332.

[21] J. Wang, M. Lu, L. Zhang, W. Chang, L. Xu and L. Hu, Effect of welding process on the microstructure and properties of dissimilar weld joints between low alloy steel and duplex stainless steel. International Journal of Minerals, Metallurgy, and Materials, 19(6)(2012) 518-524.

[22] G. Li, J. Huang and Y. Wu, An investigation on microstructure and properties of dissimilar

welded Inconel 625 and SUS 304 using high-power CO2 laser. International Journal of Advanced Manufacturing Technology, 76(2014) 1203–1214.

[23] P. Kah, M. Shrestha, and J. Martikainen, Trends in joining dissimilar metals by welding. Applied Mechanics and Materials, 440(2014) 269-276.

[24] K.D. Ramkumar, A. Singh, S. Raghuvanshi, A. Bajpai, T. Solanki, M. Arivarasu, N. Arivazhagan and S. Narayanan, Metallurgical and mechanical characterization of dissimilar welds of austenitic stainless steel and super-duplex stainless steel–a comparative study. Journal of Manufacturing Processes, 19(2015) 212-232.

[25] A. Putz, V.A. Hosseini, M. W. Elin, E. Norbert and A. V. Vahid, Microstructure investigation of duplex stainless steel welds using arc heat treatment technique. Welding in the World, 64, (2020) 1135–1147.

[26] J. Xin, H. Zhang, W. Sun, C. Huang, S. Wang, J. Wei and L. Li, The microstructures and mechanical properties of dissimilar laser welding of copper and 316L stainless steel with Ni interlayer. Cryogenics, 118(2021) 103344.

[27] B. Mvola, P. Kah, J. Martikainen, Dissimilar ferrous metal welding using advanced gas metal arc welding processes. Reviews on Advanced Materials Science, 38(2)(2014) 125-137.

[28] K.Y. Benyounis, A.G. Olabi, Optimization of different welding processes using statistical and numerical approaches–A reference guide. Advances in engineering software, 39(6)(2008) 483-496.

[29] A.H. Saedi, E. Hajjari, and S.M. Sadrossadat, Microstructural characterization and mechanical properties of TIG-welded API 5L X60 HSLA steel and AISI 310s stainless steel dissimilar joints. Metallurgical and Materials Transactions, 49(2018) 5497–5508.

[30] T.W. Nelson, J.C. Lippold and M.J. Mills, Investigation of boundaries and structures in dissimilar metal welds. Science and Technology of Welding and Joining, 3(5)(1998) 249-255.

[31] S. Kou, Y.K. Yang, Fusion-boundary macro segregation in dissimilar filler welds. Welding Journal, 86(10)(2007) 303 - 312

[32] K. Subodh, A.S. Shahi, Effect of heat input on the microstructure and mechanical properties of gas tungsten arc welded AISI 304 stainless steel joints. Materials and Design, 32(2011) 3617-3623.

[33] API 5L Pipe Line--HEBEI HUAYANG STEEL PIPE CO., LTD (hbhuayang.com)

[34] Duplex Stainless Steel (DSS): Definition, Grades, Composition, Properties, and Applications